



## Biochemical and Spectroscopic Studies of the Electronic Structure and Reactivity of a Methyl–Ni Species Formed on Methyl-Coenzyme M Reductase

Mishtu Dey,<sup>‡</sup> Joshua Telser,<sup>†,§</sup> Ryan C. Kunz,<sup>‡</sup> Nicholas S. Lees,<sup>†</sup> Stephen W. Ragsdale,<sup>‡</sup> and Brian M. Hoffman<sup>\*,†</sup>

Department of Chemistry, Northwestern University, 2145 Sheridan Road, Evanston, Illinois 60208-3113, and Department of Biochemistry, University of Nebraska-Lincoln, Lincoln, Nebraska 68588-0664

Received June 27, 2007; E-mail: bmh@northwestern.edu

Methyl-coenzyme M reductase (MCR) catalyzes the formation of methane from the methylthioether methyl-coenzyme M and coenzyme B.<sup>1</sup> The active form of MCR, denoted MCR<sub>red1</sub>, contains a nickel(I) F<sub>430</sub>, tetrapyrrole.<sup>2–4</sup> Two mechanisms have been proposed for methane synthesis: one involves an organometallic methyl–Ni(III) intermediate,<sup>5,6</sup> while the other includes a methyl radical.<sup>7</sup> A methyl–Ni intermediate has never been trapped during the reaction of MCR with native substrates, although a propyl-3-sulfonate-Ni(III)F<sub>430</sub> species has been characterized<sup>8,9</sup> and shown to undergo reactions resembling the proposed intermediate steps in methanogenesis and anaerobic methane oxidation.<sup>10,11</sup> The observation of a methyl–Ni MCR species is thus of considerable significance in terms of both biochemistry and bio-organometallic chemistry.

It was expected that the methyl–Ni(III) species formed during methanogenesis would be highly oxidizing and undergo immediate conversion to a methyl–Ni(II) state. Thus, it is surprising that reaction of MCR<sub>red1</sub> with CH<sub>3</sub>I converts the EPR spectrum of the former,  $g_{\perp} = 2.065$ ,  $g_{\parallel} = 2.24$ , to a stable axial signal,  $g_{\perp} = 2.10$ ,  $g_{\parallel} = 2.22$ , denoted MCR<sub>Me</sub> (Figure 1; 35 GHz spectra, Figure S1, Supporting Information). The  $g$  tensors of both MCR<sub>red1</sub> and MCR<sub>Me</sub> centers surprisingly are characteristic of d<sup>9</sup> metal ions with the unpaired electron (hole) primarily localized in the  $d_{x^2-y^2}$  orbital.

The rate of MCR<sub>Me</sub> formation approximates the maximum rate of methane formation from methyl–SCoM and CoBSH (4.5 s<sup>-1</sup> at 20 °C)<sup>6</sup> and is dependent on [CH<sub>3</sub>I]; the second-order rate constant, 1900 M<sup>-1</sup> s<sup>-1</sup> (inset, Figure 1), is approximately 2-fold larger than the  $k_{cat}/K_M$  for methane formation from its natural substrates (930 M<sup>-1</sup> s<sup>-1</sup> at 20 °C and 1.9 × 10<sup>4</sup> M<sup>-1</sup> s<sup>-1</sup> at 65 °C).<sup>6</sup>

To establish the nature of the Ni center of MCR<sub>Me</sub>, this state was prepared with both <sup>13</sup>CH<sub>3</sub>I and CD<sub>3</sub>I,<sup>12</sup> and we generated 2D field-frequency patterns comprising stochastic CW (<sup>13</sup>C) or pulsed<sup>13</sup> (<sup>1,2</sup>H) 35 GHz ENDOR spectra collected at multiple fields across the EPR envelope of the MCR<sub>Me</sub> isotopologues, Figure 2.<sup>14,15</sup> In the frequency range, 0–27 MHz, Figure 2, the spectra of natural-abundance MCR<sub>Me</sub> show <sup>14</sup>N ENDOR signals from the strongly coupled in-plane <sup>14</sup>N ligands of the F<sub>430</sub> macrocycle. Analysis shows the hyperfine coupling is roughly isotropic, with  $a(^{14}\text{N}) \approx 28$  MHz. The large value is characteristic of an in-plane ligand to a  $S = 1/2$  metal ion with its electron/hole in a  $d_{x^2-y^2}$  orbital, as found for the parent MCR<sub>red1</sub>,  $a(^{14}\text{N}) \approx 29$  MHz,<sup>16</sup> a propyl-3-sulfonate-Ni product ( $a(^{14}\text{N}) = 26.6\text{--}30.5$  MHz<sup>8</sup>), and MCR<sub>ox1</sub> ( $a(^{14}\text{N}) = 24.0\text{--}26.5$  MHz).<sup>17</sup>

At each field, the spectrum of <sup>13</sup>CH<sub>3</sub>MCR<sub>Me</sub> shows a single new peak, the  $\nu_+$  branch of a <sup>13</sup>C doublet with frequency,  $\nu_+ = \nu_C + A(^{13}\text{C})/2$ . The value of  $\nu_+$  increases strongly with field as the field

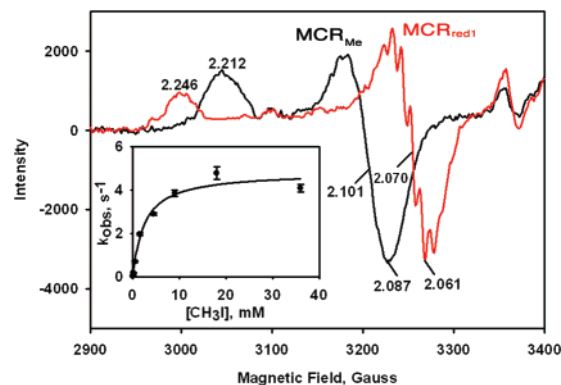


**Figure 1.** EPR spectrum of MCR<sub>Me</sub> (black) formed by incubation of 10  $\mu\text{M}$  MCR<sub>red1</sub> (red) with 1 mM CH<sub>3</sub>I in 50 mM Tris (pH 7.6) at 20 °C. The inset shows 10  $\mu\text{M}$  MCR<sub>red1</sub> converted to MCR<sub>Me</sub> by reacting with varying concentrations of CH<sub>3</sub>I in 50 mM Tris, pH 7.6 containing 0.2 mM Ti(III) citrate. The data were fit to a 2-parameter hyperbolic equation with  $k_{max}$  of  $4.8 \pm 0.3$  s<sup>-1</sup>,  $K_M$  of  $2.5 \pm 0.5$  mM, ( $k_{max}/K_M$  of  $1900 \pm 400$  M<sup>-1</sup> s<sup>-1</sup>).

is lowered from  $g_{\perp}$  to  $g_{\parallel}$ , a dependence characteristic of an axial hyperfine tensor that is coaxial with  $g$ ; simulations (Figure 2) yield the hyperfine tensor principal values,  $A_{\parallel} = a_{iso} + T = 43.0(5)$  MHz,  $A_{\perp} = a_{iso} - T = 20.0(5)$ , corresponding to  $a_{iso} = 27.7$  MHz,  $T = 7.7$  MHz. The presence of this large isotropic coupling unambiguously establishes that the CH<sub>3</sub> is covalently bound to the paramagnetic Ni(III) ion. At the same time, this coupling corresponds to only ~1% spin density in a 2s orbital on <sup>13</sup>C.<sup>18</sup>

Figure 3 presents the 2D field-frequency plot of <sup>2</sup>H( $I = 1$ ) stochastic Mims ENDOR spectra of CD<sub>3</sub>MCR<sub>Me</sub>. The <sup>2</sup>H spectra appear as doublets at frequencies,  $\nu_{\pm} = \nu_D \pm A/2$ , in which the further small<sup>19</sup> quadrupole splittings are not resolved. Simulation of the 2D <sup>2</sup>H pattern (Figure 3) shows that it is unlike the <sup>13</sup>C pattern (Figure 2) in that it is dominated by the dipolar contribution:  $A_{\perp} = -0.58$ ,  $A_{\parallel} = 1.76$  MHz ( $T = 0.78$  MHz,  $a_{iso} = 0.2$  MHz), where the unique direction is at an angle,  $\theta \approx 20^\circ$  relative to  $g_{\parallel}$ .<sup>13,20</sup>

The reaction of CH<sub>3</sub>I with the Ni(I)F<sub>430</sub> of MCR<sub>red1</sub> thus is shown by EPR/ENDOR measurements to form a Ni–CH<sub>3</sub> bond through what is formally an oxidative addition to Ni(I):



The puzzling observation that the Ni(I) ion of MCR<sub>red1</sub> and the Ni(III) ion of MCR<sub>Me</sub> both have  $d_{x^2-y^2}$  odd-electron orbitals, even though the formal electron count on Ni differs by two, is understandable through a cartoon bonding scheme for a Ni–CH<sub>3</sub> fragment, Scheme 1, similar to one presented earlier.<sup>23</sup> This scheme shows the highest two d-orbitals of the parent Ni(I) center, occupied

<sup>†</sup> Northwestern University.

<sup>‡</sup> University of Nebraska-Lincoln.

<sup>§</sup> Permanent address: Roosevelt University, Chicago, Illinois 60605.

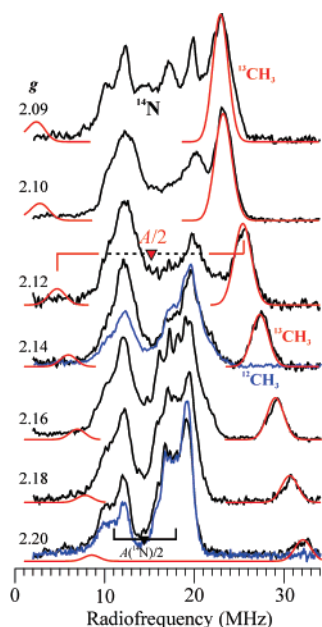


**Figure 2.** CW stochastic<sup>21</sup> 35 GHz ENDOR spectra of <sup>13</sup>CH<sub>3</sub>MCR<sub>Me</sub> (black) and <sup>12</sup>CH<sub>3</sub>MCR<sub>Me</sub> (blue; selected). The red traces are <sup>13</sup>C simulations using  $g_{\perp} = 2.095$ ,  $g_{\parallel} = 2.221$ ,  $A_{\perp} = 20.0$ ,  $A_{\parallel} = 43.0$  MHz, **A** collinear with **g**. “Goalposts” show  $2\nu(^{13}\text{C}, ^{14}\text{N})$ ; triangle indicates  $A(^{13}\text{C}, ^{14}\text{N})/2$ . Conditions: 2 K; microwave frequency, 35.089 GHz; power  $\approx 1 \mu\text{W}$ ; 100 kHz field modulation amplitude,  $\sim 1.3$  G; sample time, 1 ms; delay time, 1.5 ms; rf time, 2.0 ms, 200 scans.

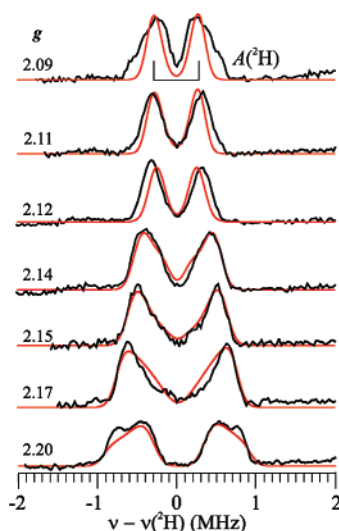


**Figure 3.** Mims stochastic 35 GHz ENDOR spectra for CD<sub>3</sub>MCR<sub>Me</sub>. Simulations (red):  $A_{\perp} = -0.58$ ,  $A_{\parallel} = 1.76$  MHz,  $\theta = 18^{\circ}$ . Conditions: 2 K; frequency, 34.811 GHz;  $\pi/2$ -pulse, 50 ns;  $\tau = 500$  ns;  $t_{\text{rf}}$ , 60  $\mu\text{s}$ , with random selection (“hopping”) of rf and baseline correction;<sup>22</sup> 20 scans.

by three electrons, and the empty  $sp^n$  hybrid of the hypothetical  $\text{CH}_3^+$  with which this center reacts to form the Ni(III)-CH<sub>3</sub> fragment. The  $sp^n$  forms a strong two-electron bond with Ni  $d_{z^2}$  in which the bonding orbital primarily is associated with C, corresponding to a strong transfer of charge to C. The antibonding orbital lies above the  $d_{x^2-y^2}$  orbital, unoccupied.

This picture explains why the odd-electron orbital is largely unperturbed by the oxidative addition reaction and why the transfer of spin to CH<sub>3</sub> is minimal: the Ni–C two-electron bond does not involve the odd electron, which in effect is a spectator to the reaction! The change in  $g$ -values can be assigned primarily to changes in the d-orbital splittings.

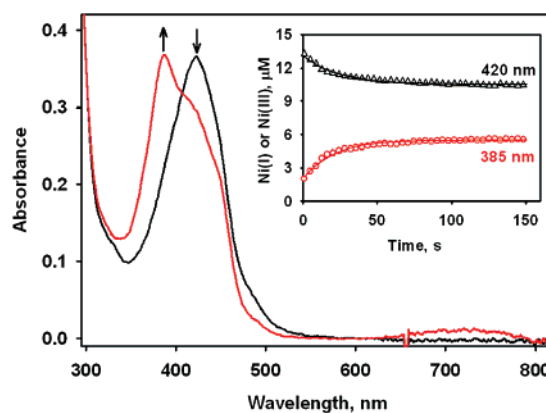
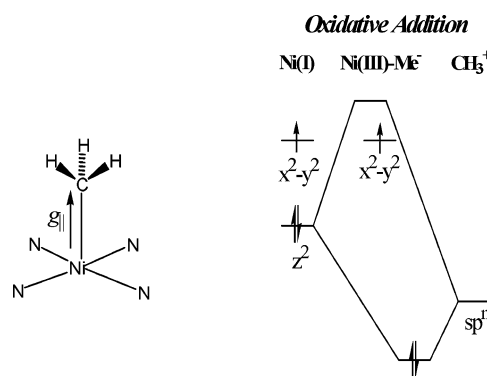


**Figure 4.** Conversion of MCR<sub>Me</sub> (black) to MCR<sub>red1</sub> (red). The inset shows decay of MCR<sub>Me</sub> ( $\Delta$ , 420 nm,  $k(\text{decay}) = 0.035(5) \text{ s}^{-1}$ ); formation of MCR<sub>red1</sub> ( $\circ$ , 385 nm,  $k(\text{form}) = 0.044(5) \text{ s}^{-1}$ ). Conditions: MCR<sub>Me</sub> formed in situ (10  $\mu\text{M}$  MCR<sub>red1</sub> plus 100  $\mu\text{M}$  MeI in 50 mM Tris, pH 7.6) was treated with 10 mM HSCoM at 25 $^{\circ}$ .

#### Scheme 1



Two competing mechanisms can contribute to the small transfer of spin to the axial ligand of a  $d_{x^2-y^2}$  odd-electron metal ion: the low-symmetry environment of the Ni ion in F<sub>430</sub> can introduce a small degree of mixing between  $d_{x^2-y^2}$  and  $d_{z^2}$  and a resulting positive spin density ( $\rho_n$ ) in the  $sp^n$  orbital on C; the  $d_{x^2-y^2}$  spin can polarize the Ni–C bond, introducing negative spin density on C. The resultant  $\rho_n$  yields a spin density in the 2s orbital of carbon,  $\rho_s = \rho_n/(n + 1)$  and an isotropic coupling,  $a(^{13}\text{C}) = \rho_s a_0(^{13}\text{C})$ , where  $a_0(^{13}\text{C}) \approx 3770$  MHz is the coupling for a single 2s electron;<sup>18</sup> experiment then yields,  $|\rho_s| \approx 0.01$ .

Considering the <sup>2</sup>H ENDOR data, the fact that the isotropic interaction is small is consistent with the minimal transfer of spin to CH<sub>3</sub> revealed by the <sup>13</sup>C ENDOR results (small  $\rho_n$ ), and suggests that the dipolar hyperfine interaction with <sup>2</sup>H is dominated by the through-space interaction with the Ni spin. In fact, the <sup>13</sup>C and <sup>2</sup>H hyperfine interactions can be self-consistently described<sup>24</sup> by the bonding in a Ni(III)–CH<sub>3</sub> fragment (Scheme 1) if we take a Ni–C bond length of 1.9–2.0 Å, C–H bond length of 1.0 Å, hybridization at C of  $n \approx 2-3$ , and  $\rho_n \approx +0.04$ . This interpretation can be examined with DFT computations.

If MCR<sub>Me</sub> is a catalytic intermediate in methanogenesis and anaerobic methane oxidation, it should react with HSCoM to make methyl–SCoM and should undergo proton and electron transfers to form methane. For these reactions to be catalytic, MCR<sub>red1</sub> must be regenerated during this process. When the CH<sub>3</sub>–Ni(III) species was reacted with HSCoM, MCR<sub>red1</sub> was regenerated with a rate constant of 0.044 s<sup>−1</sup> (Figure 4) forming methyl–SCoM, as demonstrated by MS. Furthermore, addition of CoBSh to MCR<sub>Me</sub> led to the formation of the CoB–SS–CoM heterodisulfide product, on the basis of MS coupled with MS–MS, and methane (Figure

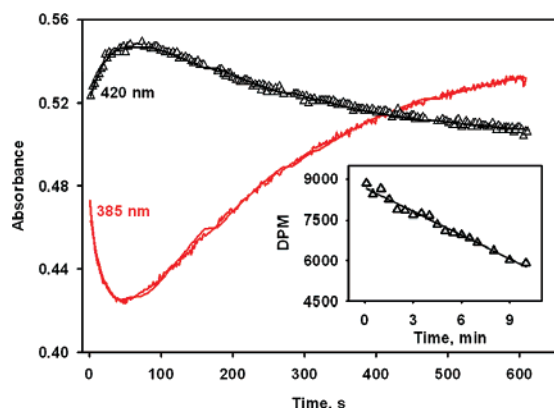


**Figure 5.** Formation of  $\text{MCR}_{\text{Me}}$  from  $\text{MCR}_{\text{red1}}$  and regeneration of  $\text{MCR}_{\text{red1}}$  by reaction of  $\text{MCR}_{\text{Me}}$  with Ti(III) citrate.  $\text{MCR}_{\text{red1}}$  ( $10 \mu\text{M}$ ) was reacted with  $50 \mu\text{M}$   $\text{CH}_3\text{I}$  in  $50 \text{ mM}$  Tris, pH 7.6 in the presence of  $0.1 \text{ mM}$  Ti(III) citrate. Timecourses:  $\text{MCR}_{\text{red1}}$ , red trace,  $385 \text{ nm}$ ;  $\text{MCR}_{\text{Me}}$ ,  $420 \text{ nm}$ , open triangles. Fit to a three-component sequential reaction gave absorbance changes at  $385 \text{ nm}$ ,  $k_1 = 0.038(2) \text{ s}^{-1}$ ,  $k_2 = 0.0047(2) \text{ s}^{-1}$ ; absorbance changes at  $420 \text{ nm}$ ,  $k_1 = 0.033(4) \text{ s}^{-1}$ ,  $k_2 = 0.0045(3) \text{ s}^{-1}$ . The inset shows  $\text{CH}_4$  formation from  $\text{MCR}_{\text{Me}}$  with Ti(III) citrate.  $\text{MCR}_{\text{red1}}$  ( $50 \mu\text{M}$ ) was reacted with  $1 \text{ mM}$   $^{14}\text{CH}_3\text{I}$  in  $50 \text{ mM}$  Tris, pH 7.6 with  $0.1 \text{ mM}$  Ti(III) citrate;  $10 \mu\text{L}$  aliquots of reaction mixture were quenched in THF at indicated times. Data was fit to a linear equation; specific activity was  $0.0048 \text{ U mg}^{-1} \text{ MCR}_{\text{red1}}$  with  $k = 0.044 \text{ s}^{-1}$ .

S3). These are the products of the reaction with the native substrates. Methane formation was shown by a steady-state experiment in which  $^{14}\text{CH}_3\text{-Ni(III)}$  (generated from  $^{14}\text{CH}_3\text{I}$ ) was reacted with  $\text{HSCoM}$  to build up methyl- $\text{SCoM}$ , at which point no methane was formed; then, upon incubation with  $\text{CoBSH}$ , methane was formed with a specific activity of  $0.046 \text{ U mg}^{-1} \text{ MCR}_{\text{red1}}$  (Figure S4). When corrected to saturating methyl- $\text{SCoM}$  concentrations, the rate constant would be  $1.1 \text{ s}^{-1}$ , similar to the typical rate of methane formation ( $4.5 \text{ s}^{-1}$  at  $20 \text{ }^\circ\text{C}$ ).<sup>6</sup> Thus, the methyl-Ni intermediate can be converted to methyl- $\text{SCoM}$ , regenerating active  $\text{MCR}_{\text{red1}}$  and, in the presence of  $\text{CoBSH}$ , can generate methane.

The low-potential reductant Ti(III) citrate is known to reduce  $\text{MCR}_{\text{ox1}}$  in vitro to active  $\text{MCR}_{\text{red1}}$ .<sup>3,4</sup> Figure 5 shows that  $\text{MCR}_{\text{Me}}$  also can undergo reduction by Ti(III) citrate to completely regenerate active  $\text{MCR}_{\text{red1}}$ , producing methane with a specific activity of  $0.046 \text{ U mg}^{-1} \text{ MCR}_{\text{red1}}$  ( $k_{\text{cat}}$  of  $0.011 \text{ s}^{-1}$ ) (inset, Figure 5). In this reaction,  $\text{MCR}_{\text{Me}}$  is generated in situ in the first phase of the reaction and then converted by Ti(III)-citrate to  $\text{MCR}_{\text{red1}}$ . Thus, the  $\text{CH}_3\text{-Ni(III)}$  species can undergo conversion to methane and regenerate  $\text{MCR}_{\text{red1}}$  in the presence of a low potential reductant (and a proton from solvent).

Support for the intermediacy of a methyl-Ni(III) intermediate during methanogenesis previously relied primarily on studies of inorganic models. Methane formation from the reaction of Ni(I)-derivatives of  $\text{F}_{430}$  and activated methyl donors like methylsulfonium ions has been observed<sup>25</sup> and a methyl-Ni(II) form of the pentamethyl ester of  $\text{F}_{430}$  has been characterized by NMR methods.<sup>26</sup> Furthermore, reaction of Ni(I)-octaethylisobacteriochlorin (a structural cousin of  $\text{F}_{430}$ ) with alkyl halides generates alkyl-Ni(III) species that undergo reduction to the alkyl-Ni(II), subsequent protonolysis yielding the alkane.<sup>27</sup> The work described here is consistent with

the intermediacy of the methyl-Ni species in methane formation, while the ENDOR measurements have characterized the methyl-Ni species long postulated to be the central catalytic intermediate of MCR.

**Acknowledgment.** This work has been supported by the NIH (Grant HL 13531, B.M.H.; Grant 1P20RR17675, S.W.R.) and Department of Energy (Grant DE-FG03-ER20297, S.W.R.).

**Supporting Information Available:** Four figures showing EPR and ENDOR spectra, mass spectra, and a methane assay. This material is available free of charge via the Internet at <http://pubs.acs.org>.

## References

- Abbreviations: methyl-coenzyme M (methyl- $\text{SCoM}$ ), 2-(methylthio)ethanesulfonic acid; coenzyme B (CoBSH), *N*-7-mercaptoheptanoyl-threonine phosphate; ENDOR, electron nuclear double resonance; mass spectrometry, MS.
- Ermiler, U.; Grabarse, W.; Shima, S.; Goubeaud, M.; Thauer, R. K. *Science* **1997**, *278*, 1457–1462.
- Goubeaud, M.; Schreiner, G.; Thauer, R. *Eur. J. Biochemistry* **1997**, *243*, 110–114.
- Becker, D. F.; Ragsdale, S. W. *Biochemistry* **1998**, *37*, 2369–2647.
- (a) Signor, L.; Knuppe, C.; Hug, R.; Schweizer, B.; Pfaltz, A.; Jaun, B. *Chem.-Eur. J.* **2000**, *6*, 3508–3516. (b) Grabarse, W. G.; Mahler, F.; Duin, E. C.; Goubeaud, M.; Shima, S.; Thauer, R. K.; Lamzin, V.; Ermiler, U. *J. Mol. Biol.* **2001**, *309*, 315–330.
- Hornig, Y.-C.; Becker, D. F.; Ragsdale, S. W. *Biochemistry* **2001**, *40*, 12875–12885.
- Pelmenschikov, V.; Blomberg, M. R. A.; Siegbahn, P. E. M.; Crabtree, R. H. *J. Am. Chem. Soc.* **2002**, *124*, 4039–4049.
- Hinderberger, D.; Piskorski, R. P.; Goenrich, M.; Thauer, R. K.; Schweiger, A.; Harmer, J.; Jaun, B. *Angew. Chem., Int. Ed.* **2006**, *45*, 3602–3607.
- Goenrich, M.; Mahler, F.; Duin, E. C.; Bauer, C.; Jaun, B.; Thauer, R. K. *J. Biol. Inorg. Chem.* **2004**, *9*, 691–705.
- Kunz, R. C.; Hornig, Y.-C.; Ragsdale, S. W. *J. Biol. Chem.* **2006**, *281*, 34663–34676.
- Dey, M.; Kunz, R. C.; Lyons, D. M.; Ragsdale, S. W. *Biochemistry* **2007**, submitted for publication.
- MCR was isolated from *Methanothermobacter marburgensis* and  $\text{MCR}_{\text{red1}}$  was generated in vivo and purified as previously described.<sup>10</sup> UV-visible, stopped flow, and EPR experiments were performed as described previously.<sup>10,11</sup> MeNiMCR was formed by reacting  $10 \mu\text{M}$   $\text{MCR}_{\text{red1}}$  with  $1 \text{ mM}$   $\text{CH}_3\text{I}$  in  $50 \text{ mM}$  Tris-HCl, pH 7.6.
- Schweiger, A.; Jeschke, G. *Principles of Pulse Electron Paramagnetic Resonance*; Oxford University Press: Oxford, U.K., 2001.
- 35 GHz EPR/ENDOR instrumentation and ENDOR analysis procedures have been described in ref 15.
- Lees, N. S.; Chen, D.; Walsby, C. J.; Behshad, E.; Frey, P. A.; Hoffman, B. M. *J. Am. Chem. Soc.* **2006**, *128*, 10145–10154.
- Telsler, J.; Hornig, Y.-C.; Becker, D. F.; Hoffman, B. M.; Ragsdale, S. W. *J. Am. Chem. Soc.* **2000**, *122*, 182–183.
- Harmer, J.; Finazzo, C.; Piskorski, R.; Bauer, C.; Jaun, B.; Duin, E. C.; Goenrich, M.; Thauer, R. K.; Van Doorslaer, S.; Schweiger, A. *J. Am. Chem. Soc.* **2005**, *127*, 17744–17755.
- Weil, J. A.; Bolton, J. R.; Wertz, J. E. *Electron Paramagnetic Resonance: Elementary Theory and Practical Applications*; John Wiley & Sons, Inc: New York, 1994; Table G.4.
- Lucken, E. A. C. In *Nuclear Quadrupole Coupling Constants*; Academic Press: New York, 1969; pp 217–247.
- The appearance of well-resolved doublets is shown to result from Mims hyperfine suppression in the vicinity of the deuteron Larmor frequency (Figure S2, Supporting Information).
- Lee, H.-I.; Igarashi, R. Y.; Laryukhin, M.; Doan, P. E.; Dos Santos, P. C.; Dean, D. R.; Seefeldt, L. C.; Hoffman, B. M. *J. Am. Chem. Soc.* **2004**, *126*, 9563–9569.
- Epel, B.; Arieli, D.; Baute, D.; Goldfarb, D. *J. Magn. Reson.* **2003**, *164*, 78–83.
- Craft, J. L.; Hornig, Y.-C.; Ragsdale, S. W.; Brunold, T. C. *J. Am. Chem. Soc.* **2004**, *126*, 4068–4069.
- Manikandan, P.; Choi, E.-Y.; Hille, R.; Hoffman, B. M. *J. Am. Chem. Soc.* **2001**, *123*, 2658–2663.
- Lin, S. K.; Jaun, B. *Helv. Chim. Acta* **1992**, *75*, 1478–1490.
- Lin, S. K.; Jaun, B. *Helv. Chim. Acta* **1991**, *74*, 1725–1738.
- Lahiri, G. K.; Stolzenberg, A. M. *Inorg. Chem.* **1993**, *32*, 4409–4413.

JA074556Z